Available online at www.sciencedirect.com
ScienceDirect
Analytical Biochemistry 374 (2008) 133–142
ANALYTICAL BIOCHEMISTRY
www.elsevier.com/locate/yabio

Interactions of fusidic acid and elongation factor G with lipid membranes

Jaana Muhonen [a], Jukka Vidgren [a], Anne Helle [a], Gebrenegus Yohannes [a], Tapani Viitala [b], Juha M. Holopainen [c,*], Susanne K. Wiedmer [a,*]

[a] *Laboratory of Analytical Chemistry, Department of Chemistry, 00014 University of Helsinki, Finland*
[b] *KSV Instruments, 00380 Helsinki, Finland*
[c] *Helsinki Eye Lab, Department of Ophthalmology, University of Helsinki, 00290 Helsinki, Finland*

Received 28 August 2007
Available online 14 October 2007

Abstract

Fusidic acid (FA) is a potent antibiotic and blocks the protein synthesis by binding to elongation factor G (EF-G) directly. Here we hypothesized that the antibiotic activity of FA would be potentiated by several orders of magnitude if both FA and EF-G would be residing in the lipid membranes and, hence, the probability of interaction would transform from three-dimensional to two-dimensional. Such detailed information could lead to more effective therapeutic interventions if they are understood on a molecular level. Interactions between FA and various lipid membranes composed of 1-palmitoyl-2-oleyl-*sn*-glycero-3-phosphocholine (POPC) and cholesterol (Chol) were studied by capillary electrochromatography (CEC). The influence of the lipid vesicle size—sonicated liposomes and liposomes extruded through 30-, 50-, and 100-nm filters—on the packing of vesicles on the silica capillary surface was investigated by CEC and dissipative quartz crystal microbalance. The CEC results evidenced that FA interacts with and resides in phospholipid membranes. Likewise, monolayer, asymmetrical flow field flow fractionation, and CEC studies confirmed that EF-G is hydrophobic and incorporated into POPC and POPC/Chol membranes. Including EF-G in phospholipid vesicles did not improve the binding of FA to the membranes.

Keywords: Capillary electromigration techniques; Elongation factor G; Field flow fractionation; Fusidic acid; Liposomes; Quartz crystal microbalance

Fusidic acid (FA)[1] is a hydrophobic, steroid-based, narrow spectrum antibiotic derived from *Fusidium coccineum.* It is a weak acid (pK_a of 5.7) and is mostly ionized in plasma and tissue at the physiological pH of 7.4 [1]. FA is used mainly to treat bacterial infections caused by gram-positive (G^+) bacteria such as *Staphylococcus aureus.* Yet it is also effective against gram-negative (G^-) *Neisseria* species as well as corynebacteria, nocardia, and anaerobes [2].

The synthesis of new proteins in living cells occurs on the ribosome. The elongation factor G (EF-G) plays an important role in the elongation phase of the protein synthesis by catalyzing the translocation of the peptidyl transfer RNA (tRNA) from the A-site to the P-site of the ribosome. EF-G is bound to the ribosome in a complex with guanosine triphosphate (GTP). After hydrolysis of GTP to guanosine 5′-diphosphate (GDP) and followed by translocation, EF-G–GDP is dissociated from the ribosome. The crystal structure of EF-G has been solved [3,4].

* Corresponding authors. Fax: +358 9 191 50253.
E-mail addresses: juha.holopainen@hus.fi (J.M. Holopainen), susanne.wiedmer@helsinki.fi (S.K. Wiedmer).

[1] *Abbreviations used:* FA, fusidic acid; EF-G, elongation factor G; tRNA, transfer RNA; GTP, guanosine triphosphate; GDP, guanosine 5′-diphosphate; CEC, capillary electrochromatography; POPC, 1-palmitoyl-2-oleyl-*sn*-glycero-3-phosphocholine; Chol, cholesterol; QCM, quartz crystal microbalance; AsFlFFF, asymmetrical flow field flow fractionation; Hepes, 4-(2-hydroxyethyl)-1-piperazineethanesulfonic acid; GMP–PNP, guanosine 5′-(β-γ-imido)triphosphate; BGE, liposome solvent and electrolyte; EOF, electroosmotic flow; LUV, large unilamellar vesicle; HPLC, high-performance liquid chromatography; CZE, capillary zone electrophoresis; QCM-Z, quartz crystal microbalance based on impedance analysis; 2D, two-dimensional; 3D, three-dimensional.

0003-2697/$ - see front matter
doi:10.1016/j.ab.2007.10.014

Cryo-transmission electron microscopy studies have shown that the binding of EF-G–GTP to the ribosome and the following hydrolysis of GTP causes large structural changes in the ribosome and in EF-G [5,6]. FA blocks protein synthesis by inhibiting EF-G directly [7]. FA binds with high affinity to the EF-G-GDP after the hydrolysis of GTP and prevents the release of EF-G–GDP complex from the ribosome [8], thereby stalling protein synthesis. There is no structural evidence for the existence of an EF-G–GDP–FA complex without the presence of ribosomes. Yet indirect evidence for FA–EF-G complex has been presented [9].

For FA to reach intracellular EF-G, it first must interact with bacterial membranes. Then it may either randomly diffuse within the bacteria to an EF-G-containing location or remain partitioned within the membrane. In the latter case, EF-G must be attached to the bacterial membranes, where it may interact with FA. Ribosomes are able to interact directly with lipid membranes [10]. Accordingly, detailed knowledge of FA–lipid membrane and EF-G–membrane interactions is essential to understand, and possibly to enhance, the antimicrobial activity of FA and similar agents. The aim of this study is to fill this gap.

The hydrophobicity of compounds is linked directly to their membrane partitioning. The high capacity of FA for tissue penetration has been ascribed to the surface activity [11], and the lipid solubility of this drug has been studied only recently [12]. We have studied the partitioning of FA into lipid bilayers and FA–phospholipid interactions both experimentally—by means of capillary electrochromatography (CEC), differential scanning calorimetry, and fluorescence spectroscopy—and through molecular dynamics simulations [12]. We showed that FA partitioned readily into the lipid bilayer and possibly was enriched in lipid rafts. This may be followed by the association of EF-G–GDP with FA-enriched lipid domains.

Here we extend our previous study and further elucidate interactions between FA and various lipid membranes composed of 1-palmitoyl-2-oleyl-*sn*-glycero-3-phosphocholine (POPC) and cholesterol (Chol) by CEC. In addition, the influence of the lipid vesicle size on the packing of vesicles on the silica capillary surface was investigated by CEC and dissipative quartz crystal microbalance (QCM). The interaction of EF-G with lipid membranes was assessed by monolayer, asymmetrical flow field flow fractionation (AsFlFFF), and CEC studies. The presence of EF-G in the lipid membrane on the retention of FA was of specific interest. The goal was to acquire more information about the interactions of FA and/or EF-G with lipid membranes.

Materials and methods

Materials

4-(2-Hydroxyethyl)-1-piperazineethanesulfonic acid (Hepes), POPC, GDP, guanosine 5′-(β-γ-imido)triphosphate (GMP–PNP), atenolol, dichlorphenamide, and FA were purchased from Sigma Chemical (St. Louis, MO, USA). β-Cholesterol was obtained from Avanti Lipids (Alabaster, AL, USA). Testosterone, $MgCl_2$, and pH solutions (7 and 10) used for calibrating the pH meter were purchased from Merck (Darmstadt, Germany). Sodium hydroxide (1.0 M) and nitric acid (1.0 M) were obtained from FF Chemicals (Yli Ii, Finland), methanol was obtained from Mallinckrodt Baker (Deventer, The Netherlands), and chloroform was obtained from Rathburn Chemicals (Walkerburn, UK). Distilled water was further purified with a Millipore Water Purification System (Millipore, Molsheim, France). EF-G was expressed and purified as described previously and was kindly donated by Suparna Sanyal (Department of Cell and Molecular Biology, Uppsala University) [13].

Buffer and sample preparation

Hepes-containing buffer solution, with an ionic strength of 20 mM and pH 7.4 (adjusted with 1.0 M sodium hydroxide), was used as liposome solvent and electrolyte (BGE) solution. Before use, the BGE was filtered through a 0.45-μm syringe filter (Gelman Sciences, Ann Arbor, MI, USA). The samples for CEC studies were prepared from stock solutions of atenolol, aldosterone, testosterone, and dichlorphenamide (1.0–2.8 mg ml^{-1} in methanol). For CEC runs, the concentrations of the analytes in the injected sample were 40 μg ml^{-1} all in 5:95% (v/v) methanol/BGE solution. The concentration of FA, when used as an analyte, was 1 mM. The electroosmotic flow (EOF) in the capillaries was measured using 5 to 7.5% methanol in BGE solution as a neutral marker.

The stock solution of EF-G in water (400 μM) was diluted to 200 μM with 0.02% Na-azide and further diluted to 196, 167, 54, 30, 20, 10, 5, 2.5, or 1.25 μM into phospholipid solutions in BGE. The numbers of EF-G molecules per phospholipid molecule were then 1:0.1, 1:1, 1:12.5, 1:25, 1:50, 1:100, 1:200, 1:400, and 1:800, respectively. The pure EF-G sample was diluted with BGE solution to 4.8 μM. The stock solutions of GDP and GMP–PNP were made in BGE in the concentration of 4 mM, and final concentrations in the coating solutions were 200 to 300 μM (and the final concentration for $MgCl_2$ was 5 mM). Phospholipid dispersions were extruded through a 50-nm membrane before the addition of EF-G, GDP, GMP–PNP, or $MgCl_2$.

POPC, Chol, and FA stock solutions in chloroform and EF-G, GDP, and GMP–PNP were stored in a freezer. All other solutions were stored in a refrigerator.

Liposome preparation

Liposome vesicles were prepared from POPC, Chol, and FA stock solutions (20 mM in chloroform). Liposomes were prepared as described previously [14]. Appropriate amounts of the lipid stock solutions in chloroform were mixed to obtain the desired compositions. The resulting

mixture was evaporated to dryness under a stream of compressed air, and traces of solvent were removed by evacuation under reduced pressure (8–100 mbar) for 16 h. The lipid residues were hydrated in the indicated buffer at 60 °C to yield multilamellar vesicles with a lipid concentration of 1 mM, and the vesicles were maintained at this temperature for 60 min with subsequent shaking. During hydration, the vesicle-containing solution was vortexed four or five times. The resulting dispersion was processed to large unilamellar vesicles (LUVs) by extrusion 19 times through 30-, 50-, or 100-nm pore size polycarbonate filters (Millipore, Bedford, MA, USA) using a LiposoFast extruder and a pneumatic actuator with an external pressure of 3.5 bar (Avestin, Ottawa, Canada).

Sonicated liposomes were made by using a microtip Branson Sonifier 250 sonicator (Branson Ultrasonic, Danbury, CT, USA) with the following setups: output control 1 to 3 and duty cycles 10 to 50. The lipid solution was kept in an icewater bath during sonication. Sonication was continued until the lipid solution became clear, and the total sonication time was approximately 10 to 15 min depending on the ratio of POPC, Chol, and FA.

Capillary electrophoresis

A Hewlett–Packard ^{3D}CE system (Agilent, Waldbronn, Germany) equipped with a diode array detector (wavelengths 200 and 245 nm) was used for the electrophoretic analyses. Uncoated fused silica capillaries were obtained from Composite Metal Services (Worcestershire, UK). Dimensions of the capillaries were 50 μm i.d. (375 μm o.d.), length of capillary to detector 30 cm, and total length 38.5 cm.

For studies with POPC/Chol/FA coatings, the fresh capillary was preconditioned by rinsing the capillary at a pressure of 930 to 940 mbar for 10 min with 0.5 M nitric acid and for 15 min with water. Phospholipid coating was applied to the capillary inner surface as follows. After preconditioning, the capillary was rinsed for 10 min with a 1-mM liposome dispersion at 930 to 940 mbar and then incubated with the liposome dispersion for 15 min. Finally, the capillary was rinsed with BGE solution for 10 min before running the analytes. New fresh capillaries were employed for each measurement series of different phospholipid coatings.

Before coating the capillary with EF-G liposome dispersions, the electrophoretic mobility of FA was determined in the uncoated capillary ($n = 4$). After these runs, the capillary was rinsed with water for 10 min and then coated with EF-G–liposome dispersions as described above.

CEC separation conditions were as follows: voltage 20 kV in the POPC/Chol/FA studies and 30 kV in the EF-G studies; temperature of samples and capillary cassette 25 °C; and sample injection 2 s at 50 mbar. Before each injection, the capillary was rinsed for 1 min with the liposome dispersion and for 2 min with the BGE solution. Separations of analytes were repeated eight times except for EF-G coatings (four times). The quality of the BGE solution was ensured by the change of the buffer vials after every ninth run.

Quartz crystal microbalance

A KSV multifrequency QCM-Z500 (KSV Instruments, Helsinki, Finland) was used to monitor adsorption of liposome vesicles prepared from POPC, Chol, and FA on a Si-coated quartz crystal. The QCM-Z500 instrument-measuring principle is based on impedance analysis. The contacting adsorbed layer and bulk liquid phase create mechanical perturbations in the quartz crystal and alter its electrical characteristics. The QCM-Z500 instrument allows one to record the impedance of the 5-MHz ($n = 1$) crystal and its adlayers at several overtone frequencies of 15, 25, 35, 45, and 55 MHz (ns = 3, 5, 7, 9, and 11, respectively). Thus, by measuring the impedance over the crystal and using equivalent circuit analysis, one can relate the electrical impedance of the quartz crystal to the mechanical properties of the adsorbed layer and contacting liquid phase.

If the layer adsorbed on the crystal surface is rigid and homogeneous, the normalized frequency changes recorded for all overtone frequencies superimpose on each other and the frequency shift is proportional to the mass of the adsorbed material. Under this situation, the Sauerbrey equation derived for rigid films can be applied [15]:

$$\Delta m = -\frac{C}{n}\Delta f, \tag{1}$$

where C (= 17.7 ng/(cm^2 Hz) at $f = 5$ MHz) is the mass sensitivity constant and n (= 1, 3, 5, ...) is the overtone number.

For adsorbed layers that do not fulfill the above requirements, there is a deviation from the Sauerbrey equation because the added mass is soft and/or not properly attached to the underlying surface; therefore, it is not fully coupled with the crystal oscillation. In such cases, measuring the electrical properties of the quartz crystal and the added layers at multiple overtones is useful to determine the mechanical properties of the adsorbed layer. By using equivalent circuit modeling, one can then access the mechanical properties of the added layers on the quartz crystal such as mass, density, thickness, and the viscoelastic properties [16,17]. However, in this study, it was not necessary to use this more elaborate modeling because the adsorbed layers were considered to be in a range where the Sauerbrey equation could be applied. The data analysis and calculations of thickness and adsorbed masses in this study were performed using the proprietary QCM Impedance Analysis software (KSV Instruments, version 3.11).

Field flow fractionation

The AsFlFFF channel was constructed in-house in a manner similar to that used by other groups [18–21]. A regenerated cellulose acetate ultrafiltration membrane with a molar mass cutoff of 10 kDa (DSS-RC70PP, Nakskov,

Denmark) was laid on top of the porous frit. A Mylar spacer with a thickness of 500 μm and the channel shape cutout was placed between the ultrafiltration membrane and the upper glass plate. The nominal channel dimensions were 38 cm × 2 cm × 500 μm. A high-performance liquid chromatography (HPLC) pump (model PU-980, Jasco International, Tokyo, Japan) was used to move the carrier liquid. Samples were introduced into the channel at 1.0 ml min^{-1} for 5 to 10 min by another HPLC pump. During the injection–relaxation–focusing period, the carrier liquid was delivered from both the front and back of the channel at a flow rate of 3.3 ml/min for 12 min. The outlet flow from the channel was monitored with a UV/visible detector (HP1050 model 79853 C, Tokyo, Japan) at 280 nm. Capillary Teflon tubes (0.5 mm i.d.), restrictors, and three-way valves (V101T, Upchurch Scientific, Oak Harbor, WA, USA) were used to control the carrier liquid flows. An Agilent ChemStation for LC and LC/MS (Palo Alto, CA, USA) was used for data acquisition.

Radioactivity measurements

POPC/Chol (80:20 mol%) 50-nm vesicles, containing 1 μCi of [^{14}C]POPC, were prepared as described above. After the addition of purified EF-G to the extruded vesicles, the samples were fractionated by AsFlFFF and the radioactivity associated with the EF-G-enriched fraction was examined by liquid scintillation counting (WinSpectral 1414 Liquid Scintillation Counter, Wallac, Turku, Finland). The results are expressed as means (± SD) from triplicate wells.

Monolayer studies

Penetration of EF-G into POPC/Chol (80:20 molar ratio) monolayers was measured using circular Teflon-coated wells (subphase volume 2400 μl). Surface pressure (π) was monitored with a Wilhelmy wire attached to a microbalance (μTroughS, Kibron, Helsinki, Finland) and connected to a Pentium personal computer. The monolayer was spread on an air–buffer interface by the dropwise addition of lipid–chloroform (1 mg/ml) spreading solution from a Hamilton syringe to desired initial surface pressures (π_0). The resulting monolayers were allowed to equilibrate for 10 min before the addition of EF-G (2.5 μl, stock solution 400 μM) into the subphase. The addition of an equal volume of buffer did not change π. The increment in πfrom the initial surface pressures (π_0) after the addition of EF-G was complete in less than 90 min, and the difference between π_0 and the value observed after binding of EF-G into the film (π_f) was taken as Δπ. All measurements were performed at ambient temperature (~ 24 °C). The data are represented as Δπ versus π_0.

Calculations

The retention factor in CEC has been studied recently by many groups [22,23]. Rathore and Horváth [24] introduced a retention factor k'' as an analogue of the chromatographic retention factor under conditions of CEC experiments. k'' measures the magnitude of the retention due to reversible binding of analytes to the CEC stationary phase and holds for both uncharged and charged analytes. For cases of phospholipid-coated capillaries and interaction studies, Wiedmer and coworkers [25] transformed the equation of k'' into the form

$$k'' = t_m\left(\frac{1}{t_{eo}} + \frac{1}{t_{m'}} - \frac{1}{t_{eo'}}\right) - 1, \quad (2)$$

where t_m and t_{eo} are the migration times of the analyte and the EOF marker in a coated capillary, respectively, and $t_{m'}$ and $t_{eo'}$ are the migration times of the analyte and the EOF marker in an uncoated capillary, respectively. In the current study, Eq. (2) was used to measure the retention behavior of analytes in POPC/Chol/FA-coated capillaries. Capillary zone electrophoretic (CZE) runs were employed to determine the migration times of the analytes ($t_{m'}$) and the EOF marker ($t_{eo'}$) in an uncoated capillary.

Kenndler [26] introduced the reduced mobility (μ_i) to express the effect of the EOF on all separation parameters relevant for CZE. The reduced mobility μ_i is given by

$$\mu_i = \frac{\mu_{ep}}{\mu_{ep} + \mu_{eo}} \quad (3)$$

where μ_{ep} is the effective electrophoretic mobility of the analyte and μ_{eo} is the EOF in the coated capillary. In the current study, the reduced mobility was used to illustrate the interaction of FA with EF-G in EF-G–liposome-coated capillaries.

Results and discussion

Given the lipid membrane partitioning of FA [12], the aim of this study was to provide a more thorough understanding of FA–lipid and EF-G–lipid interactions. For FA to inhibit protein synthesis in bacteria, it needs to bind to EF-G; accordingly, this needs to take place in the plane of the lipid bilayer. Thus, detailed information of EF-G–lipid membrane interactions is needed. In this work, we explored the effects of FA on EF-G partitioning to lipid membranes. Various lipid compositions and vesicle sizes were tested in CEC for choosing an appropriate liposome composition and size for coating the capillary for the proceeding FA/EF-G study. Capillaries were coated with 30, 50, and 100 nm extruded and sonicated vesicles composed of POPC, Chol, and FA (Fig. 1). The liposome compositions investigated were POPC/Chol/FA with molar ratios of 100:0:0 mol%, 80:20:0 mol%, 60:40:0 mol%, 80:0:20 mol%, 60:0:40 mol%, 80:10:10 mol%, 60:20:20 mol%, 60:30:10 mol%, and 60:10:30 mol%. The EOFs in the coated capillaries were measured, and the organization of different sized liposomes on silica was further evaluated by QCM. The retention of some model compounds (Fig. 1) was used for evaluation of the hydrophobicity of the different lipid membranes. The interactions between EF-G and the lipid membranes were

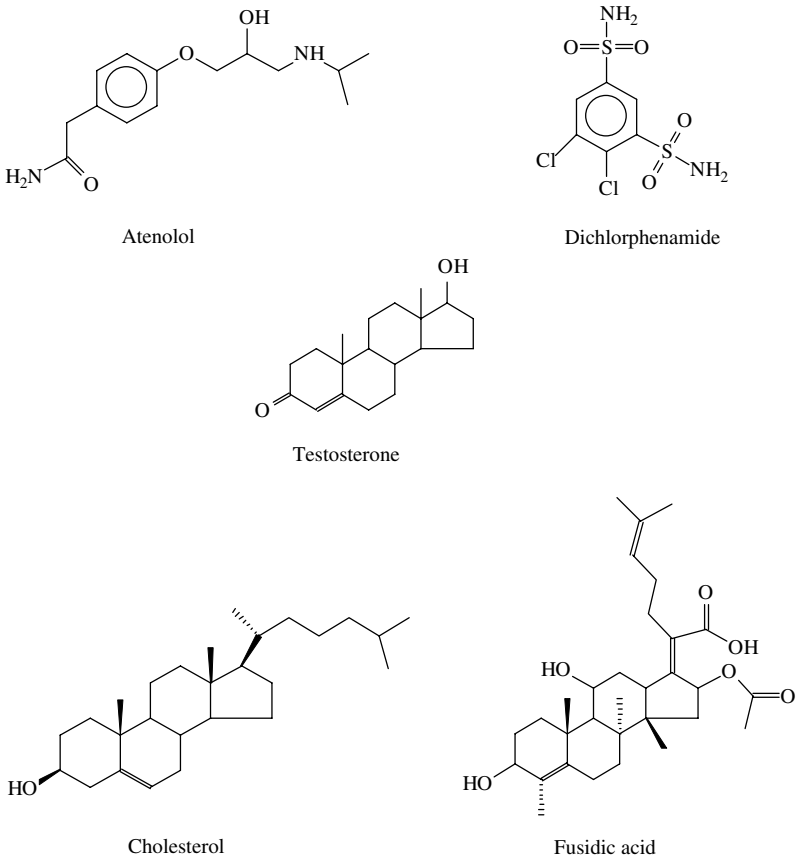

Fig. 1. Structures of studied molecules.

investigated by CEC, AsFlFFF, and monolayer studies. Finally, the interaction of FA with EF-G/lipid membranes was evaluated by CEC.

Effect of vesicle size on the EOF and liposome packing on silica

The influence of the vesicle size on the EOFs in the coated capillary was studied first. The EOF was the lowest when the capillary was coated with extruded 30-nm or sonicated vesicles, suggesting that the coating was denser with smaller vesicles than with larger vesicles (Fig. 2). EOF in the capillaries coated with 100-nm vesicles approached the EOF of the uncoated capillary, indicating that the capillary was not uniformly coated and there were still free negatively charged silanol groups on the capillary surface.

The sonicated vesicles filled the capillary surface better and gave more repeatable results compared with the larger extruded vesicles. Sonicated vesicles formed a durable coating in the capillary, but FA (as an analyte) interacted very strongly with these coatings, resulting in long migration times of FA (10–20 min). When Chol-containing sonicated liposomes were used as coating material, the interactions between FA and the membranes were very strong; FA was adsorbed onto the membrane and did not come out from the capillary at all. This observed high affinity of FA to Chol-rich membranes did not occur with capillaries coated with extruded vesicles; hence, sonicated vesicles were not a suitable choice for further studies. Extruded 30-nm vesicles coated the capillary well, but the vesicles were assumed to be too small for the proceeding EF-G studies. On the other hand, coatings formed from 100-nm vesicles were unstable, probably due to loosely packed liposomes on the surface of the capillary. In conclusion, 50-nm extruded vesicles were chosen for further studies because they resulted in coatings dense enough for EF-G studies.

To get a deeper understanding of the packing of different sized vesicles on silica, studies with a multifrequency quartz crystal microbalance based on impedance analysis (QCM-Z) were carried out. Extruded liposomes with sizes of 50 and 100 nm with POPC/Chol/FA compositions of 100:0:0, 80:20:0, 80:0:20, and 60:20:20 were compared. The results from the QCM-Z measurements are summarized in Table 1. The average of all normalized frequency shifts of all measured overtones for each liposome composition was in the range of 30 Hz or less. The standard deviations of the normalized frequency shifts also were rather small, indicating that the adsorbed layer is sufficiently thin and rigid to be analyzed by using the Sauerbrey approach. Hence, all liposome compositions formed bilayer or bilayer patches on the silica surface, and no evidence of the formation of adsorbed vesicle layers could be detected for any of the used liposome compositions.

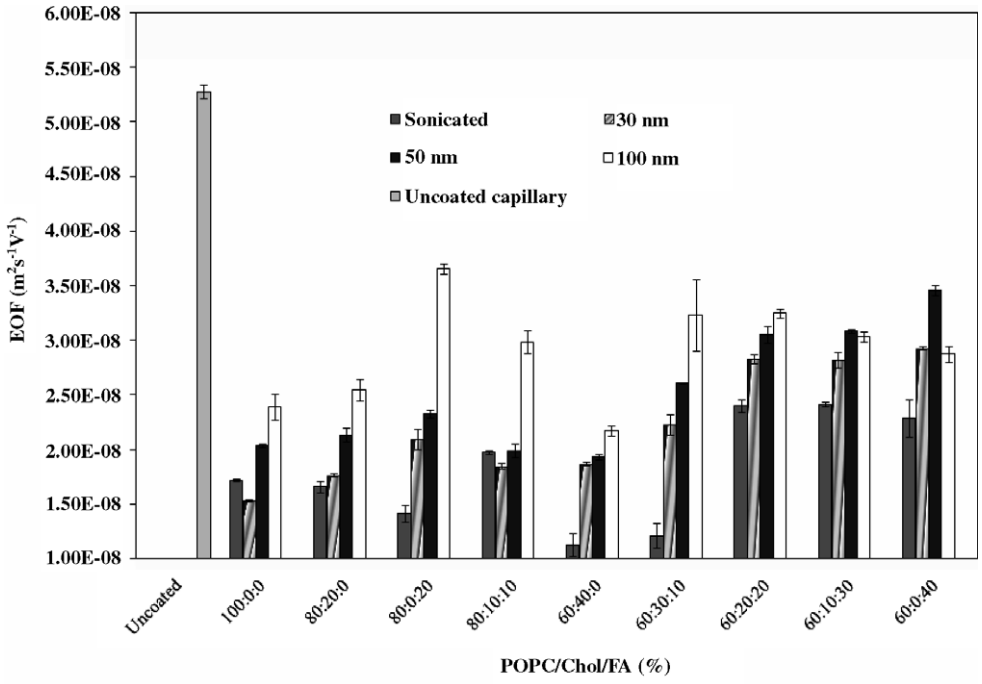

Fig. 2. EOF values in capillaries coated with extruded vesicles (membrane pore sizes were 30, 50, and 100 nm) and sonicated vesicles ($n = 8$). The vesicles consisted of POPC, Chol, and FA in different ratios.

Table 1
Summary of QCM-Z measurements

Vesicle matrix	$\Delta f/N_{AVE}$ (Hz)	$SD_{\Delta f/N}$ (Hz)	$\Delta M/\Delta A$ (ng/cm^2)	Thickness (nm)
POPC, 50 nm	28.0	2.1	497 ± 37	4.49
POPC, 100 nm	24.8	1.3	456 ± 49	4.32
POPC/Chol, 50 nm	32.1	2.1	564 ± 34	5.55
POPC/Chol,100 nm	29.1	3.1	492 ± 94	4.93
POPC/FA, 50 nm	26.2	1.8	523 ± 84	5.03
POPC/FA, 100 nm	11.9	1.3	205 ± 20	1.72
POPC/Chol/FA, 50 nm	24.5	4.2	433 ± 74	4.23
POPC/Chol/FA, 100 nm	20.8	6.6	371 ± 112	3.67

$\Delta f/N_{AVE}$ is the normalized frequency shift; $SD_{\Delta f/N}$ is the standard deviation of the normalized frequency shift; $\Delta M/\Delta A$ is the mass per area.
Note. Mass areal density of bilayer was determined by the Sauerbrey equation. Bilayer thickness was determined with an assumption of bilayer density of 1.06 g/ml.

Table 1 shows that the mass per area ($\Delta M/\Delta A$) always is larger for the smaller 50-nm liposome compositions than for the larger 100-nm compositions, indicating that more material is adsorbed on the silica surface when using the 50-nm liposome compositions than when using the 100-nm compositions. Furthermore, the modeled thickness of the formed bilayers or bilayer patches also always were larger for the 50-nm liposome compositions than for the 100-nm compositions. These QCM-Z results clearly suggest that the bilayers or bilayer patches adsorbed from the 50-nm liposome compositions are more condensed and densely packed than the layers formed from the 100-nm compositions, and this is also supported by the fact that the EOF values for the 50-nm liposome compositions always are smaller than those for the 100-nm compositions (Fig. 2). In cases where the bilayer thickness is less than 4 nm, it is considered that the adsorbed layer consists of bilayer patches because the QCM-Z technique averages over a large area (20 mm^2) and assumes that the layer is distributed homogeneously over the whole silica surface. A bilayer thickness of less than 4 to 5 nm indicates that the bilayer does not cover the whole silica surface completely due to the formation of bilayer patches because of poorer adhesion to the silica surface originating from increased repulsive interactions between the liposomes and the silica surface.

The bilayer thickness increased when Chol was added to the POPC liposome matrix (Table 1). The addition of Chol to the liposome affected only the packing of the bilayers by condensing the bilayer structure, seen as an increase in the bilayer thickness, whereas the EOF values did not change significantly. However, when FA was added to the liposome matrices, the corresponding bilayer thickness decreased and significant changes in the EOF values were seen except for the 50-nm 80:0:20 DOPC/Chol/FA liposome matrix, where the bilayer thickness and EOF value were comparable to both the pure POPC and POPC/Chol liposome matrices. The clear decrease in bilayer thickness and EOF values when introducing FA in the liposomes suggests that the adhesion of these liposomes toward the silica surface is decreased due to the negatively charged FA. However, by using Chol in the matrix with FA, one can improve the liposome adhesion in the case of the 100-nm liposomes, whereas it makes the situation worse in the case of the 50-nm liposomes. The molecular-level mechanisms behind these observed effects cannot be explained in detail at this stage.

Effect of vesicle composition on the EOF

The liposome composition studied contained POPC, Chol, and FA in various ratios (Fig. 2). Comparing membranes without and with 20 mol% of FA reveals that the surface charge of the lipid coating increased when FA was present and that this leads to higher EOF values. A further increase in the FA concentration up to 40 mol% resulted in even higher surface charge. The only exception was the coatings formed from the 100-nm vesicles; the surface charge of the POPC/Chol/FA 80:0:20 coating was higher than that of the 60:0:40 coating. This can be explained by the poorly packed surface, as evidenced by QCM. Substituting part of the POPC by Chol (cf. the 80:0:20 and 60:20:20 coatings) resulted in higher EOF values, hence in more charged surfaces (except for the 100-nm vesicles). It seems that incorporation of Chol in the membrane increases the rigidness, and alters the packing of FA in the membrane more toward the polar head group region of the membrane. The same trend was observed with coatings formed from 80:10:10 and 60:30:10 vesicles (except for the sonicated liposomes). This behavior could reflect formation of more rigid membranes, perhaps resembling the formation of the so-called liquid-ordered phase [27].

Retention of analytes

The effective electrophoretic mobility and retention factor of FA and three analytes (Fig. 1) were measured on different coatings to achieve information about the membrane properties (surface charge and hydrophobicity).

The retention factor (k'') of testosterone was solely dependent on the hydrophobicity of the phases. The data for testosterone showed that the most hydrophobic phase was that composed of 100% POPC (Fig. 3A). Very high retention was also obtained on the POPC/Chol/FA 60:40:0 coating, which was slightly surprising considering the high Chol content. This coating should show liquid-ordered behavior with relatively high lateral diffusion yet stiffness of the acyl chains [27]. In general, the addition of FA to the coatings resulted in less hydrophobic phases; however, the retention of testosterone was high on the POPC/Chol/FA 80:10:10 and 60:30:10 coatings. The retention factor of positively charged atenolol did not vary much under the experimental conditions used (data not shown).

As discussed earlier, the higher the FA concentration in the coating, the more negative was the surface charge of the phospholipid coating, showing that FA was unambiguously incorporated into the lipid membrane on the capillary wall and making the membrane surface more negative and hydrophilic. This was further evidenced by the lower retention factors for the acidic analytes dichlorphenamide and FA (Fig. 3B). On the whole, the retention of dichlorphenamide always was lower than that of testosterone.

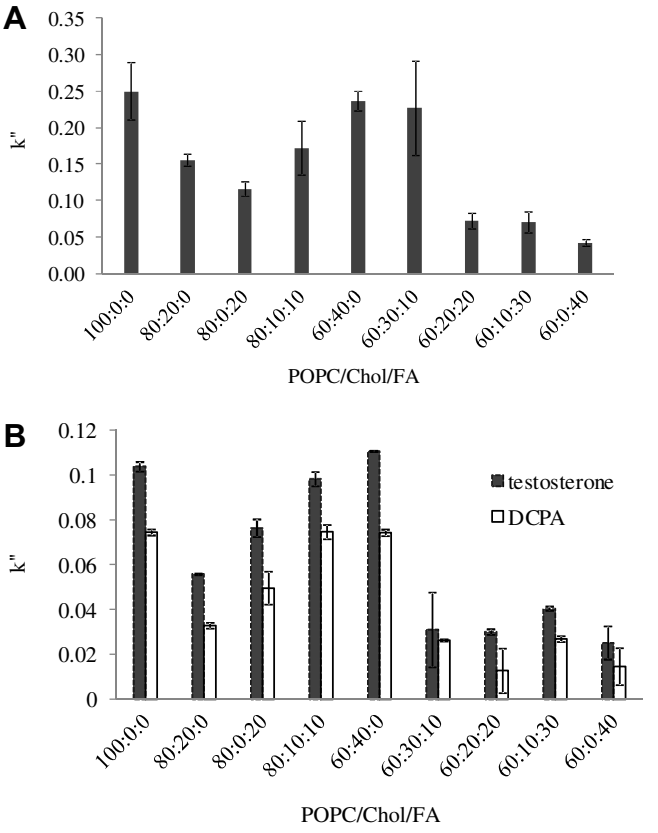

Fig. 3. Retention factors of FA (A) and testosterone and dichlorphenamide (B) in capillaries coated with 50-nm-sized POPC/Chol/FA vesicles ($n = 8$) .

The retention of FA was the highest on the most hydrophobic 100% POPC phase. Strong interactions also were seen between FA and the Chol-rich phases POPC/Chol/FA 60:40:0 and 60:30:10. On the other hand, the interaction of FA with the membrane was weaker when the membrane already was more or less saturated with FA.

Interaction between EF-G and the lipid membranes

Interactions between EF-G and the lipid membranes were studied by capillary electrophoresis using POPC/Chol 80/20 mol% and POPC 100 mol% liposomes extruded through 50-nm membranes. Liposomes mixed with various amounts of EF-G were attached to the fused silica capillary wall as described in the previous sections. Fig. 4 shows the EOF values measured in EF-G–liposome-coated capillaries. The EOF was significantly increased, and it approached the EOF of an uncoated capillary when the amount of EF-G was increased in the coating solution. EF-G consists of 700 amino acids and has a predicted molar mass of 77.4 kDa [28]. The isoelectric point of EF-G is between 4.7 and 5.1 depending on the source [28]. Hence, in the experimental conditions of pH 7.4 used, EF-G has an overall negative surface charge giving a negative EOF in the capillary. These results prove that EF-G interacts with POPC/Chol 80/20 mol% and POPC

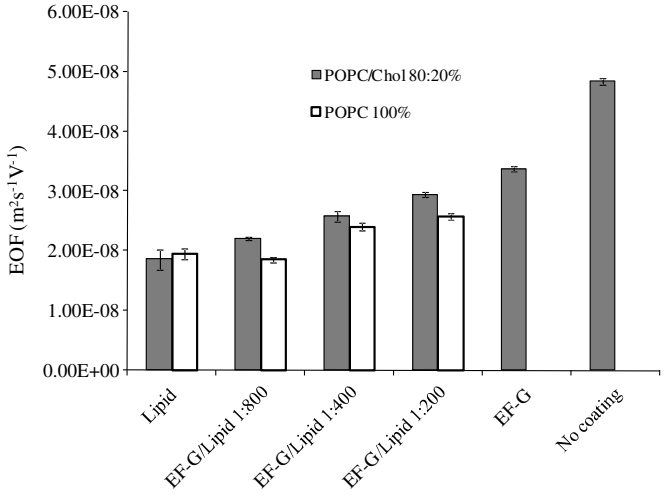

Fig. 4. EOF values in capillaries coated with POPC/Chol 80/20 mol% or POPC 100 mol% liposomes (extruded 50 nm) and EF-G–liposome solutions ($n = 4$).

100 mol% liposomes, and the good repeatabilities (cf. the standard deviations in Fig. 4) of the EOF values suggest that EF-G remains incorporated in the membrane.

Lipid monolayers residing on an air–buffer interface provide a convenient means to assess membrane partitioning of EF-G by monitoring the increase in surface pressure caused by insertion of the protein into the film. Accordingly, the hydrophobicity and lipid partitioning of EF-G was further studied by monolayer penetration studies. First, we studied the surface activity of purified EF-G in Langmuir troughs. After injection of EF-G into the subphase, there was a monotonous increase in the surface pressure up to approximately 17 mN/m (Fig. 5). A very slow subsequent increment was observed and may have been attributable to denaturation of the protein at the air–water interface [29] and/or the higher activation energy of protein adsorption to the air–water interface at high protein surface concentrations [30].

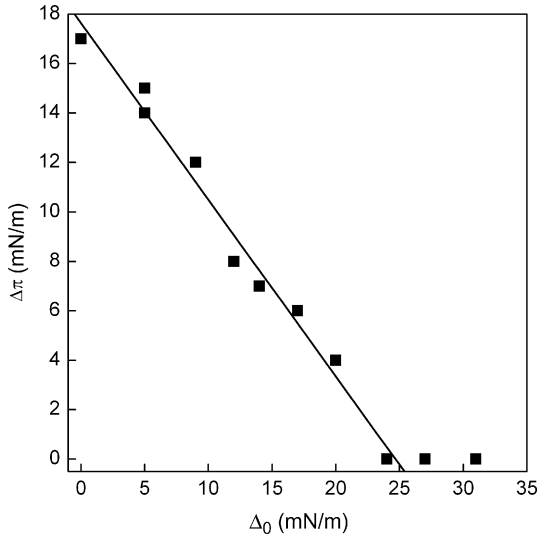

Fig. 5. Interaction of EF-G with lipid monolayers. EF-G was injected into the subphase beneath POPC/Chol monolayers spread at increasing initial surface pressures. The surface pressure was monitored until no change was seen.

To assess the partitioning of EF-G between the phospholipid monolayer and the aqueous subphase as a function of monolayer surface pressure POPC/Chol (80:20 molar ratio), monolayers were prepared in a Teflon-coated well. The initial surface pressures ranged from 0 to 31 mN/m. To these monolayers, EF-G (final concentration 0.4 μM) was injected into the subphase and the adsorption of EF-G to the interface was monitored by the change in surface pressure ($\Delta\pi$) (Fig. 5). As described previously [31], binding of a protein to a lipid membrane does not increase π; only the insertion of the protein into the monolayer will increase the value of π. The binding of EF-G to the lipid–buffer interface decreased linearly with increasing π_0 (Fig. 5); linear extrapolation of the π_0–$\Delta\pi$ curve indicated that EF-G could not penetrate the lipid monolayer surface at $\pi_0 \geqslant 25$ mN/m. At higher π_0 values, no changes in surface pressure were detected.

The AsFlFFF studies on EF-G with increasing amount of lipids were carried out to get information on the size of the proteins and on possible absorption of lipids to EF-G. The obtained hydrodynamic particle diameter of EFG was approximately 7.4 nm (Fig. 6), which is close to the size of 5.5 to 7.5 nm reported previously [32]. A shift in the protein size to 9.4 to 9.8 nm was observed with increasing amounts of lipids added (Fig. 6). To further study this change in size of the protein, POPC/Chol (80/20 mol%) 50-nm vesicles radiolabeled with [^{14}C]POPC were fractionated by AsFlFFF and the radioactivity associated with the EF-G-enriched fraction was examined by liquid scintillation counting. The results showed that there were no lipids bound to EF-G (data not shown); this was expected considering the physical properties and physiological function of the protein. The change in the size of EF-G with increasing amounts of lipids in the solution can be explained by lipid-induced aggregation and/or a conformational change of the protein [33–35].

Interactions of FA with EF-G-containing liposomes

The reduced mobility (see Eq. (3)) of FA was measured for EF-G–lipid-coated capillaries (Fig. 7). The more EF-G was added to the coating solution, the weaker was the interaction between FA and the EF-G–lipid membrane. This indicates that FA does not interact with EF-G when the EF-G is anchored in the lipid membrane. The FA binding site in EF-G probably is inside the lipid membrane or otherwise hidden, thereby leading to negligible interaction between FA and EF-G. In addition, there were no remarkable differences in the effective electrophoretic mobility of FA in the presence of Mg^{2+}, GDP, or GMP–PNP in the EF-G–lipid-coated capillaries. By performing experiments such as these, it was not possible to show direct interactions between FA and EF-G. As stated earlier, this is not unex-

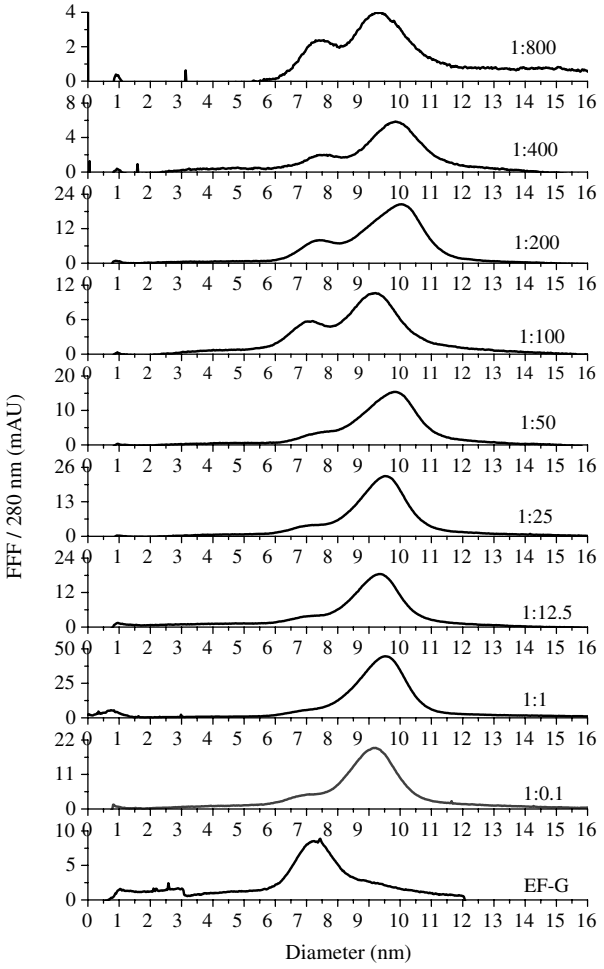

Fig. 6. Particle diameters of EF-G samples with increasing amounts of lipids measured by AsFlFFF. Sample: EFG:POPC/Chol (80:20 mol%) 1:0, 1:.01, 1:1, 1:12.5, 1:25, 1:50, 1:100, 1:200, 1:400, and 1:800 molar mixing ratios; carrier: 8.5 mM phosphate buffer (ionic strength 20 mM) and 0.02% NaN_3 (pH 7.4); relaxation focusing: flow rate at inlet 0.1 ml min^{-1}; flow inward from outlet 3.3 ml/min; injection: 1 ml/min for approximately 5 min; relaxation time: 12 min. The flow rates at the main and cross flow outlets were 0.25 ml/min and 2.77 ml/min, respectively. UV detection at 280 nm.

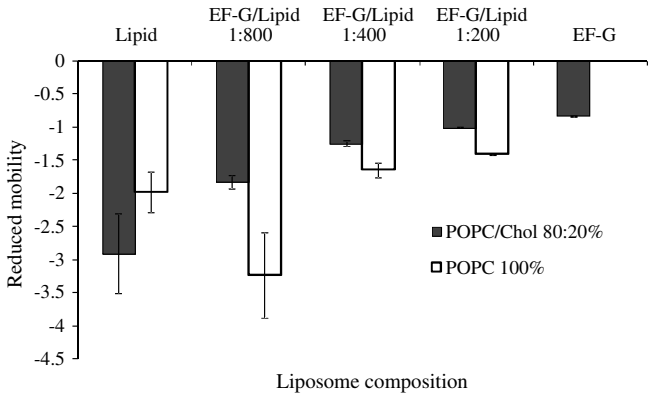

Fig. 7. Reduced mobility of FA in capillaries coated with EF-G:POPC/Chol 80/20 mol% and EF-G:POPC 100 mol% dispersions ($n = 4$).

pected because the FA binding site probably is buried in the hydrophobic core of the lipid bilayer. Finally, ribosomes probably are essential for the beneficial conformation change of EF-G, allowing the binding of FA and EF-G.

Conclusions

Using multiple approaches, we have demonstrated that FA is hydrophobic and embedded within zwitterionic lipid membranes composed of POPC and Chol. Furthermore, EF-G is hydrophobic and partitions readily within a lipid environment composed of neutral zwitterionic POPC and Chol. For FA to show efficient antibiotic activity, an important and clinically relevant factor is met. Under these experimental conditions, it was not possible to show direct interactions between FA and EF-G. The assumption here is that because both FA and EF-G are hydrophobic, they accumulate into two-dimensional (2D) platforms onto lipid membranes instead of freely floating within bacteria in a three-dimensional (3D) space. This shift from a 3D space to a 2D platform is likely to accelerate the efficiency of antibiotic activity by several orders of magnitude. Verheij and coworkers [36] estimated that this type of transition (3D → 2D) in enzymatic action of phospholipase A_2 enhances the enzyme activity approximately 10,000 times.

Acknowledgments

Financial support was received from the Academy of Finland (SA 202216, 114292) (SKW) and Sigrid Juselius Foundation, The Helsinki University Central Hospital Research Fund, and Evald and Hilda Nissi Foundation (JMH). The authors thank Dr. Jari Metso (Department of Molecular Medicine, National Public Health Institute, Helsinki) for help with the radioactivity measurements. The donation of EF-G by Dr. Suparna Sanyal (Department of Cell and Molecular Biology, Uppsala University, Sweden) is much appreciated.

References

[1] J. Turnridge, Fusidic acid pharmacology, pharmacokinetics, and pharmadynamics, Intl. J. Antimicrob. Agents 12 (1999) S23–S34.
[2] L. Verbist, The antimicrobial activity of fusidic acid, J. Antimicrob. Chemother. 25 (1990) 1–5.
[3] A. Ævarsson, E. Brazhnikov, M. Garber, J. Zheltonosova, Y. Chirgadze, S. al-Karadaghi, L.A. Svensson, A. Liljas, Three-dimensional structure of the ribosomal translocase: Elongation factor G from *Thermus thermophilus*, EMBO J. 13 (1994) 3669–3677.
[4] J. Czworkowski, J. Wang, T.A. Steitz, P.B. Moore, The crystal structure of elongation factor G complexed with GDP at 2.7 Å resolution, EMBO J. 13 (1994) 3661–3668.
[5] R.K. Agrawal, P. Penczek, R.A. Grassucci, J. Frank, Visualization of elongation factor G on the *Escherichia coli* 70S ribosome: The mechanism of translocation, Proc. Natl. Acad. Sci. USA 95 (1998) 6134–6138.
[6] R.K. Agrawal, J. Linde, J. Sengupta, K.H. Nierhaus, J. Frank, Localization of L11 protein on the ribosome and elucidation of its involvement in EF-G-dependent translocation, J. Mol. Biol. 311 (2001) 777–787.

[7] N. Tanaka, T. Kinoshita, H. Masukawa, Mechanism of protein synthesis inhibition by fusidic acid and related antibiotics, Biochem. Biophys. Res. Commun. 30 (1968) 278–283.
[8] J.W. Bodley, F.J. Zieve, L. Lin, Studies on translocation: IV. The hydrolysis of a single round of guanosine triphosphate in the presence of fusidic acid, J. Biol. Chem. 245 (1970) 5662–5667.
[9] M. Laurberg, O. Kristensen, K. Martemyanov, A.T. Gudkov, I. Nagaev, D. Hughes, A. Liljas, Structure of a mutant EF-G reveals domain III and possibly the fusidic acid binding site, J. Mol. Biol. 303 (2000) 593–603.
[10] A.J. Savitz, D.I. Meyer, Receptor-mediated ribosome binding to liposomes depends on lipid composition, J. Biol. Chem. 272 (1997) 13140–13145.
[11] S. Hansen, Intraocular penetration of fusidic acid with topical Fucithalmic, Eur. J. Drug Metab. Pharmacokinet. 10 (1985) 329–331.
[12] E. Falck, J.T. Hautala, M. Karttunen, P.K. Kinnunen, M. Patra, H. Saaren-Seppälä, I. Vattulainen, S.K. Wiedmer, J.M. Holopainen, Interaction of fusidic acid with lipid membranes: Implications to the mechanism of antibiotic activity, Biophys. J. 91 (2006) 1787–1799.
[13] S. al-Karadaqhi, A. Æversson, M. Garber, J.ZheltnosovaA. Liljas, The structure of elongation factor G in complex with GDP: Conformational flexibility and nucleotide exchange, Structure (Lond.) 4 (1996) 555–565.
[14] J.T. Hautala, M-L. Riekkola, S.K. Wiedmer, Anionic phospholipid coatings in capillary electrochromatography: Binding of Ca^{2+} to phospholipid phosphate group, J. Chromatogr. A 1150 (2007) 339–347.
[15] G. Sauerbrey, The use of quartz oscillators for weighing thin layers and for microweighing, Z. Phys. 155 (1959) 206–222.
[16] H.L. Bandey, S.J. Martin, R.W. Cernosek, A.R. Hillman, Modeling the Responses of thickness–shear mode resonators under various loading conditions, Anal. Chem. 71 (1999) 2205–2214.
[17] T. Viitala, J.T. Hautala, J. Vuorinen, S.K. Wiedmer, Structure of anionic phospholipid coatings on silica by dissipative quartz crystal microbalance, Langmuir 23 (2007) 609–618.
[18] K-G. Wahlund, A. Litzén, Application of an asymmetrical flow field–flow fractionation channel to the separation and characterization of proteins, plasmids, plasmid fragments, polysaccharides, and unicellular algae, J. Chromatogr. 461 (1989) 73–87.
[19] K-G. Wahlund, J.C. Giddings, Properties of an asymmetrical flow field–flow fractionation channel having one permeable wall, Anal. Chem. 59 (1987) 1332–1339.
[20] A. Litzén, K-G. Wahlund, Improved separation speed and efficiency for proteins, nucleic acids, and viruses in asymmetrical flow field–flow fractionation, J. Chromatogr. 476 (1989) 413–421.
[21] A. Litzén, K-G. Wahlund, Zone broadening and dilution in rectangular and trapezoidal asymmetrical flow field–flow fractionation channels, Anal. Chem. 63 (1991) 1001–1007.
[22] A.S. Rathore, Theory of electroosmotic flow, retention, and separation efficiency in capillary electrochromatography, Electrophoresis 23 (2002) 3827–3846.
[23] W. Wei, L. Guoan, Y. Chao, Calculation of retention factors for charged solutes in capillary electrochromatography, J. Sep. Sci. 24 (2001) 203–207.
[24] A.S. Rathore, C. Horváth, Chromatographic and electrophoretic migration parameters in capillary electrochromatography, Electrophoresis 23 (2002) 1211–1216.
[25] S.K. Wiedmer, M. Jussila, R.M.S. Hakala, K-H. Pystynen, M-L. Riekkola, Piperazine-based buffers for liposome coating of capillaries for electrophoresis, Electrophoresis 26 (2005) 1920–1927.
[26] E. Kenndler, Dependence of analyte separation on electroosmotic flow in capillary zone electrophoresis: Quantitative description by the reduced mobility, J. Microcol. Sep. 10 (1998) 273–279.
[27] J.H. Ipsen, G. Karlström, O.G. Mouritsen, H. Wennerström, M.J. Zuckermann, Phase equilibria in the phosphatidylcholine–cholesterol system, Biochim. Biophys. Acta 905 (1987) 162–172.
[28] V. Berchet, T. Thomas, R. Cavicchioli, N.J. Russell, A-M. Gounot, Structural analysis of the elongation factor G protein from the low-temperature-adapted bacterium *Arthrobacter globiformis* SI55, Extremophiles 4 (2000) 123–130.
[29] D.F. Cheesman, J.T. Davies, Physicochemical and biological aspects of proteins at interfaces, Adv. Protein Chem. 9 (1954) 439–501.
[30] D.E. Graham, M.C. Phillips, Proteins at liquid interfaces: I. Kinetics of adsorption and surface denaturation, Colloid Interface Sci. 70 (1979) 403–414.
[31] R.A. Demel, Y. London, W.S. Geurts van Kessel, F.G. Vossenberg, L.L. van Deenen, Specific interaction of myelin basic protein with lipids at the air–water interface, Biochim. Biophys. Acta 311 (1973) 507–519.
[32] J. Czworkowski, P.B. Moore, The conformational properties of elongation factor G and the mechanism of translocation, Biochemistry 36 (1997) 10327–10334.
[33] M. Venturoli, B. Smit, M.M. Sperotto, Simulation studies of protein-induced bilayer deformations, and lipid-induced protein tilting, on a mesoscopic model for lipid bilayers with embedded proteins, Biophys. J. 88 (2005) 1778–1798.
[34] S.M. Barnett, S. Dracheva, R.Z. Hendler, I.W. Levin, Lipid-induced conformational changes of an integral membrane prote, in: An infrared spectroscopic study of the effects of Triton X-100 treatment on the purple membrane of *Halobacterium halobium* ET1001, Biochemistry 35 (1996) 4558–4567.
[35] U. Johanson, A. Ævarsson, A. Liljas, D. Hughes, The dynamic structure of EF-G studied by fusidic acid resistance and internal revertants, J. Mol. Biol. 258 (1996) 420–432.
[36] H.M. Verheij, A.J. Slotboom, G.H. de Haas, Structure and function of phospholipase A_2, Rev. Physiol. Biochem. Pharmacol. 91 (1981) 91–203.